Supplementary information

Sequential structural evolution triggered by O-O dimerization in oxygen-redox reactions

Xiang-Mei Shi, Masashi Okubo, Atsuo Yamada*

Department of Chemical System Engineering, School of Engineering, The University of Tokyo, Hongo 7-3-1, Bunkyo-ku, Tokyo 113-8656, Japan

* Correspondence to: yamada@chemsys.t.u-tokyo.ac.jp

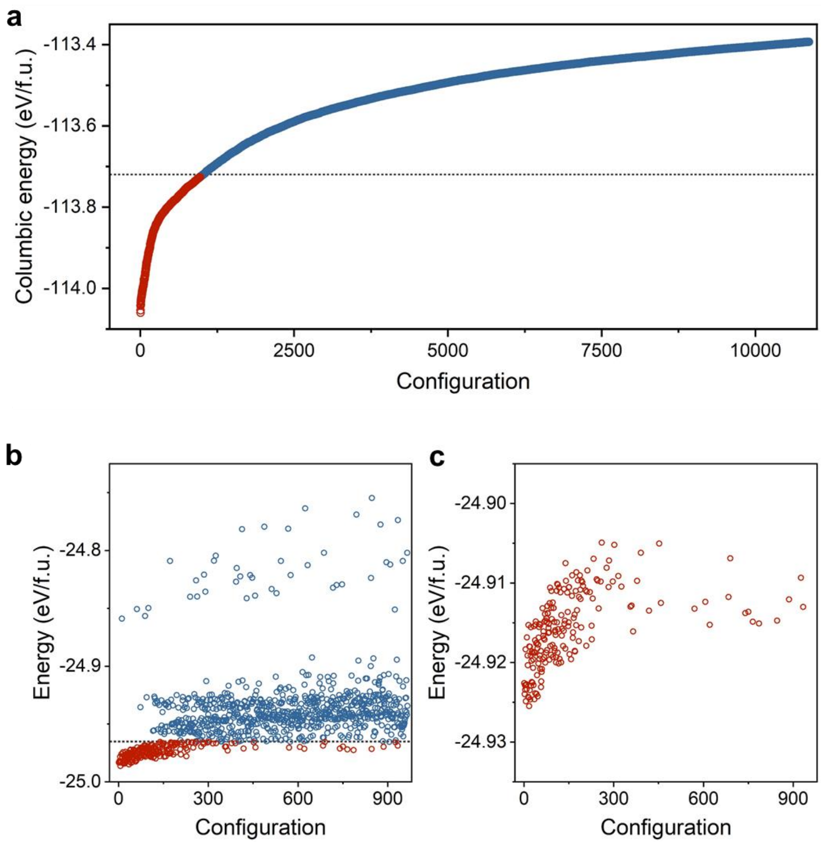

Supplementary Figure 1. Multi-step structural screening procedure for $Li_{1.2}Ni_{0.13}Co_{0.13}Mn_{0.54}O_2$. **a,** The Coulombic potential energies of all possible cationic orderings based on the pristine lattice. **b,** DFT+U energies for the screened configurations from the first step, where a rough set of geometry optimization criteria is applied. **c,** Total energies of 200 configurations calculated by the thorough optimization (DFT+U with an advanced set of parameters). Blue points represent all considered configurations while the configurations with red points are selected to conduct the next screening step.

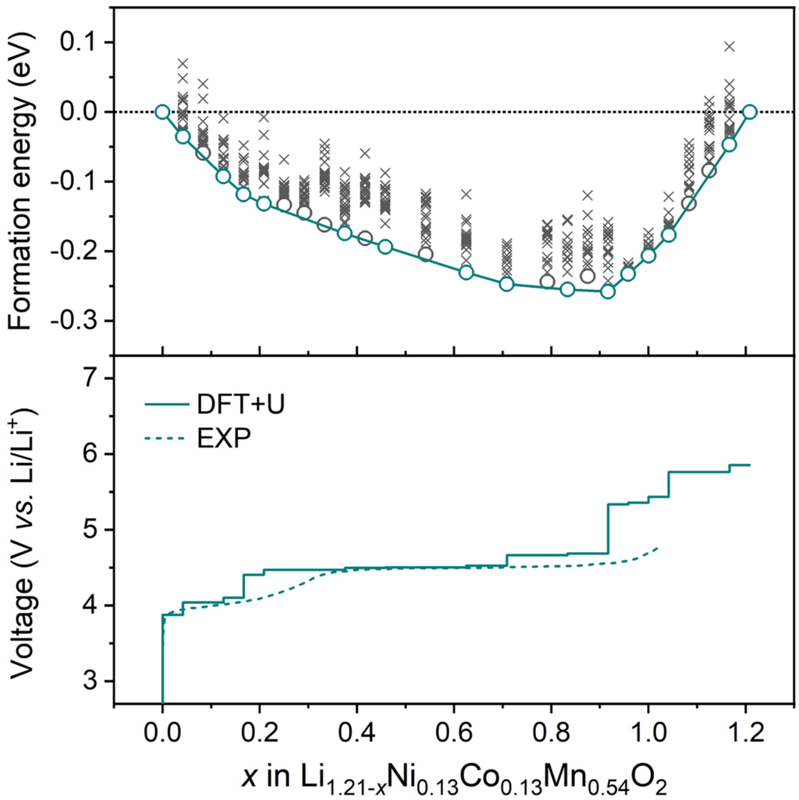

Supplementary Figure 2. Convex-hull and voltage profile of $Li_{1.2\text{-}x}Ni_{0.13}Co_{0.13}Mn_{0.54}O_2$ calculated based on the parent structure at $x = 0$. The experimental charge curve at first-cycle is compared with our result.

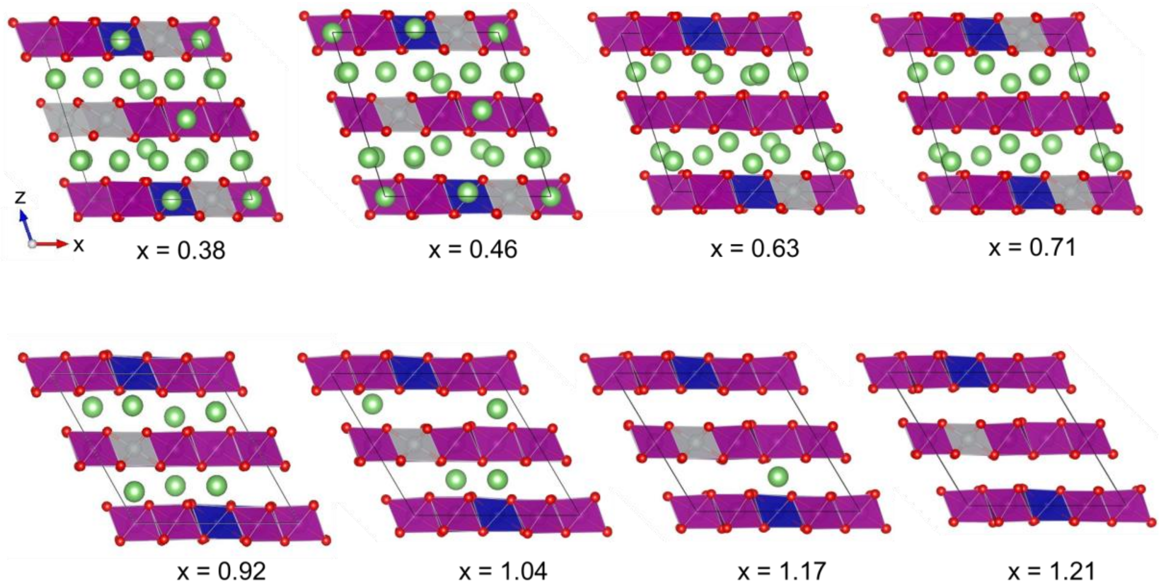

Supplementary Figure 3. Typical charged structures of $Li_{1.2-x}Ni_{0.13}Co_{0.13}Mn_{0.54}O_2$ with preserving the pristine lattice.

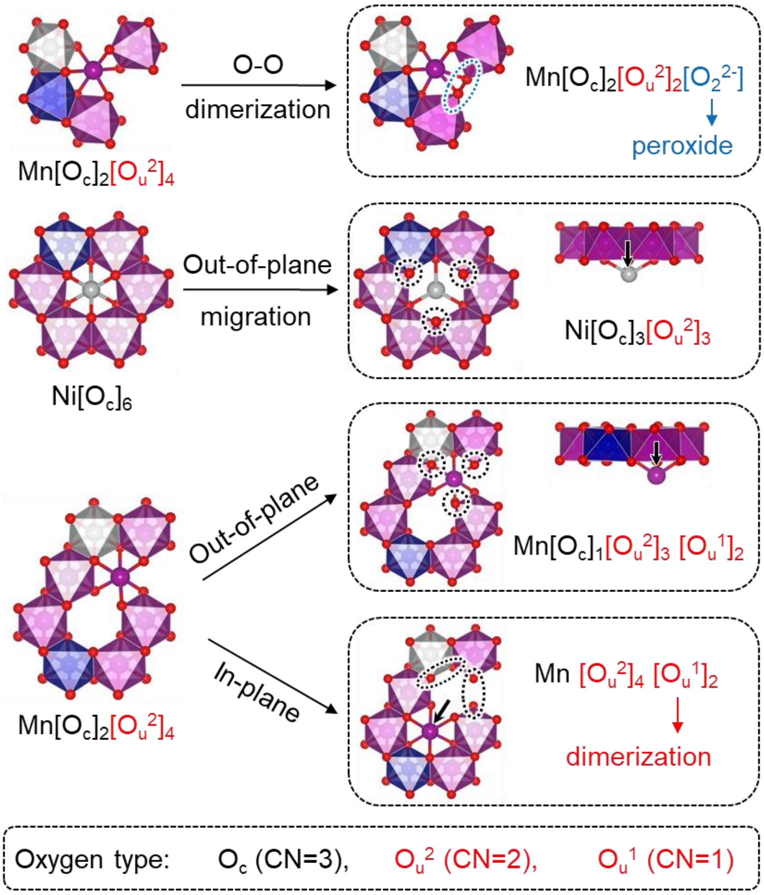

Supplementary Figure 4. Illustration of the change in the coordination environment of oxygen after O-O dimerization and different cases of TM migration. The atomic structure at x = 0.92 is put as the representative example. In terms of the coordination number (CN) for oxygen bonding to TM ions, three oxygen types are classified to describe the local structural change. O-O dimerization decreases the amount of O_u and TM migration creates less coordinated oxygen (O_u^1) or new undercoordinated oxygen (O_u^2).

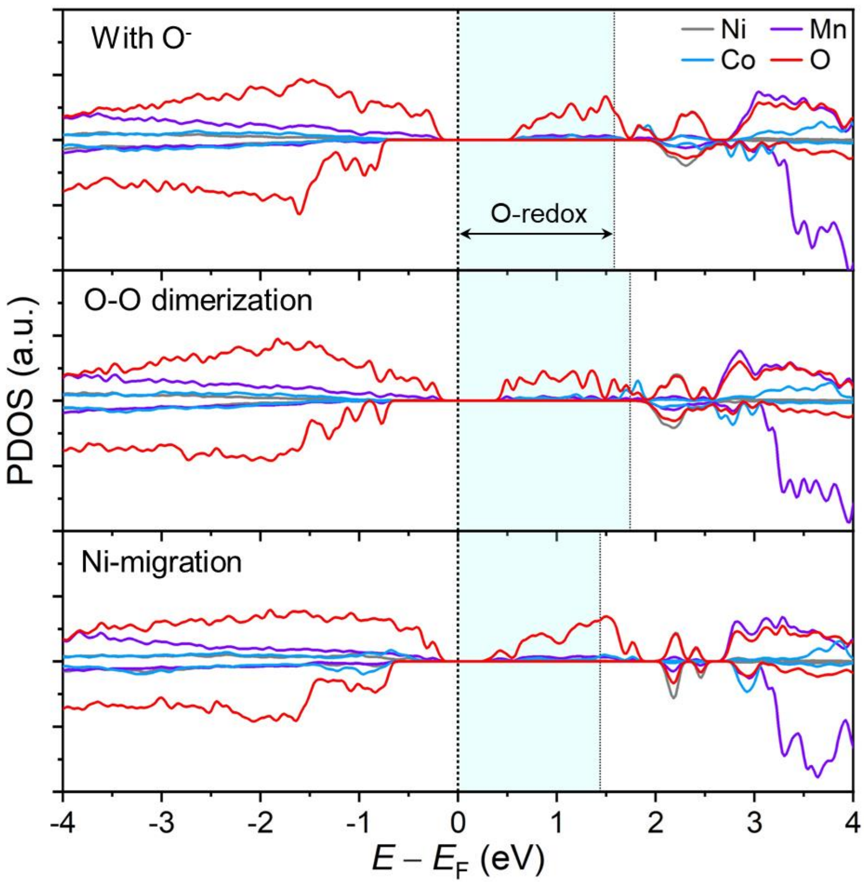

Supplementary Figure 5. Calculated PDOS of $Li_{0.29}Ni_{0.13}Co_{0.13}Mn_{0.54}O_2$. The shaded region indicated the same amount of hole states triggered by the oxygen oxidation.

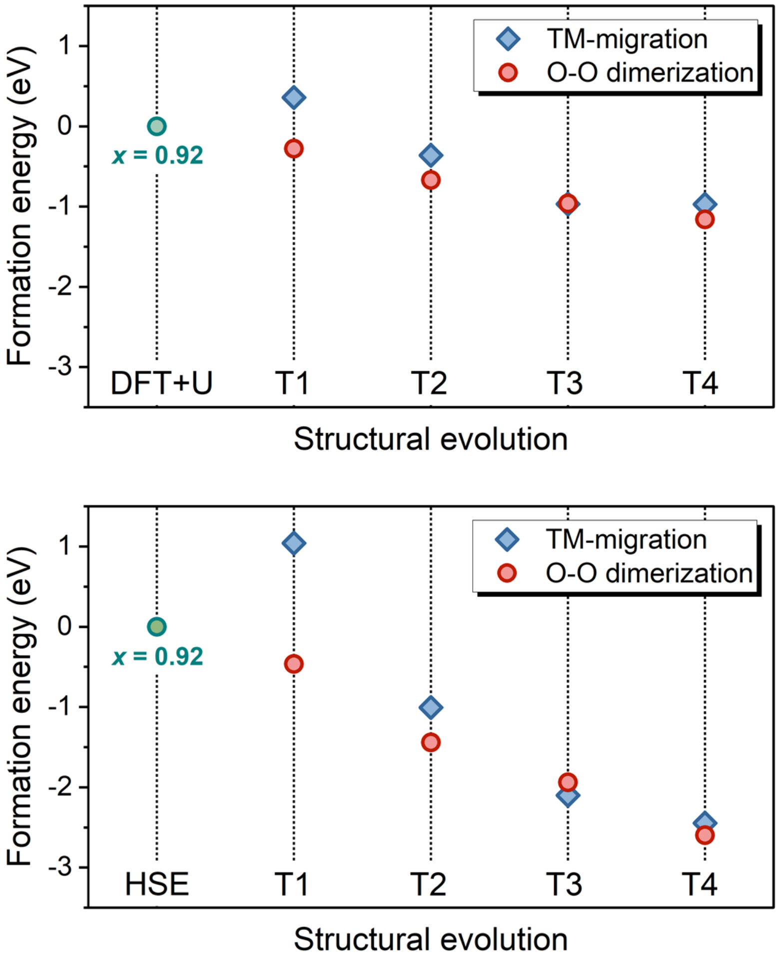

Supplementary Figure 6. Comparing DFT+U and HSE results of formation energies calculated for the structural evolution at $x = 0.92$.

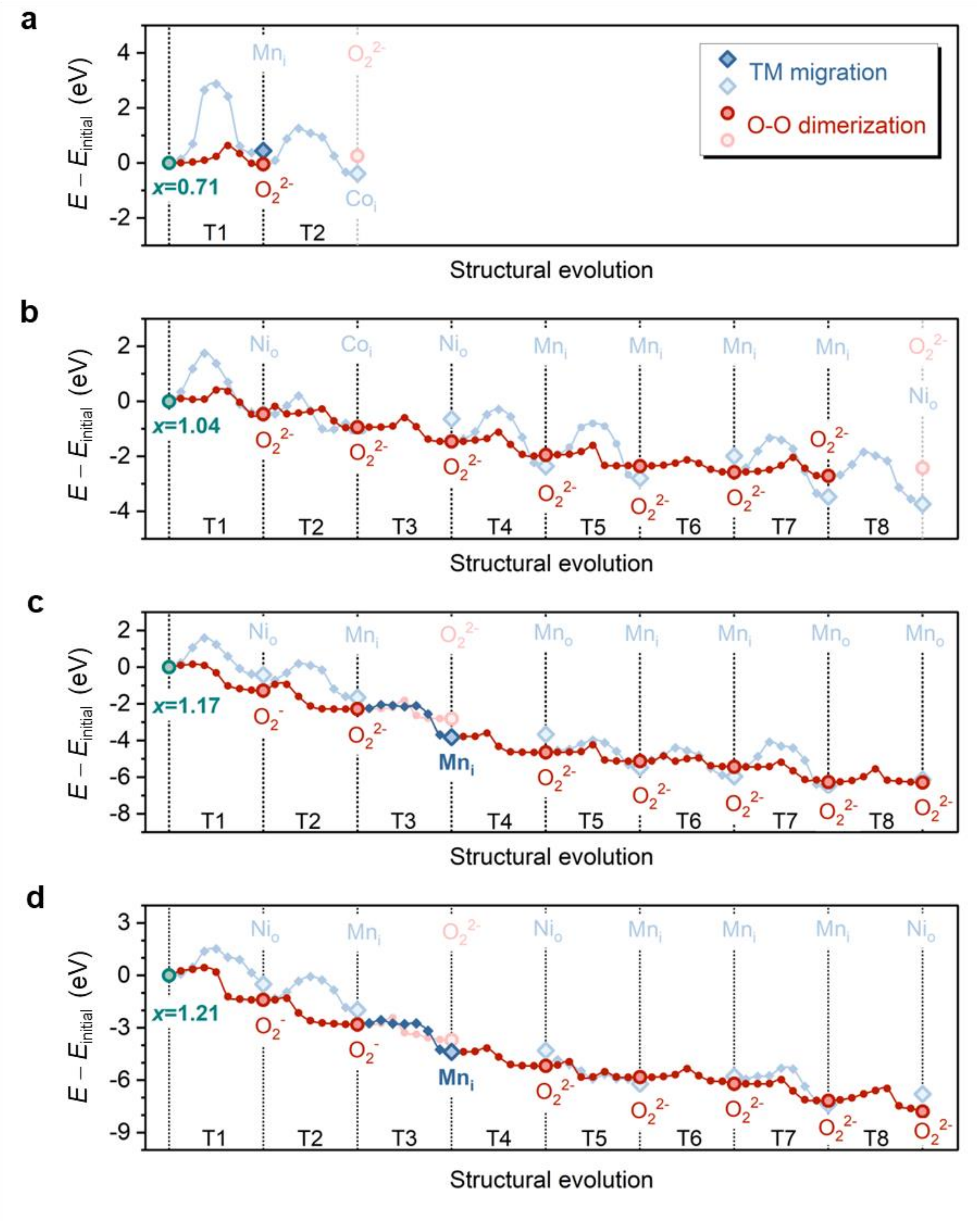

Supplementary Figure 7. Energy landscapes of the structural evolution at **a)** x = 0.71, **b)** x = 1.04, **c)** x = 1.17 and **d)** x = 1.21 (extended version of Figure 5d).

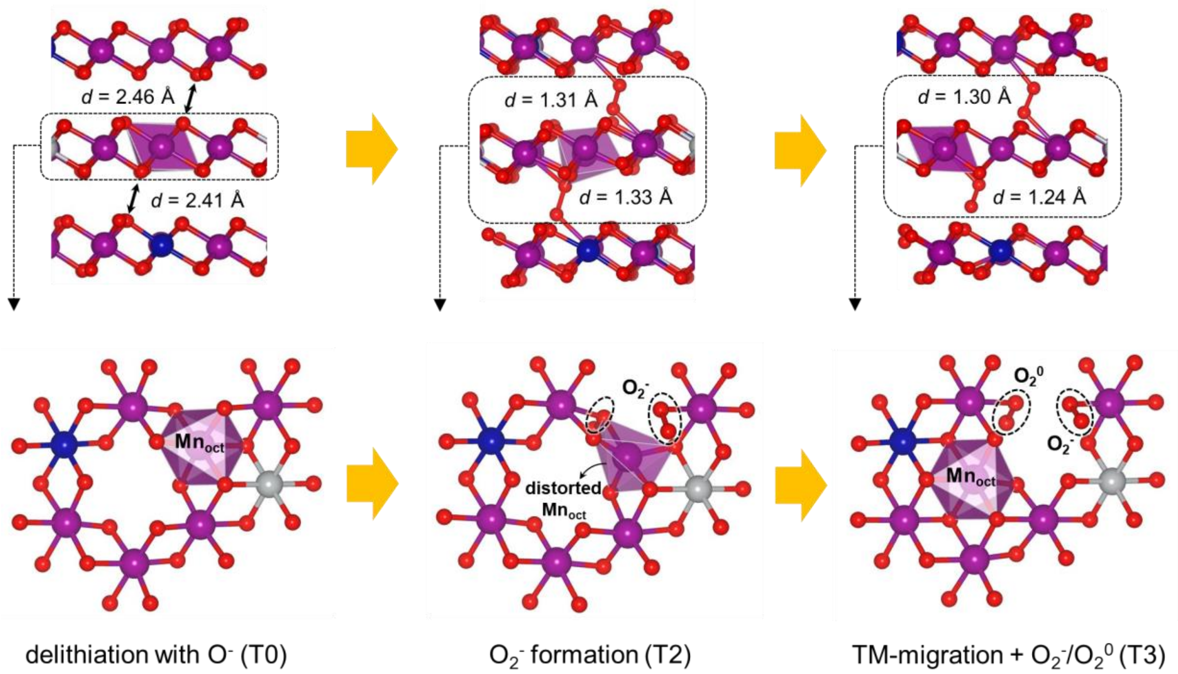

Supplementary Figure 8. Structural illustration of Mn migration (in-plane) process triggered by the superoxide formation (at x = 1.21).

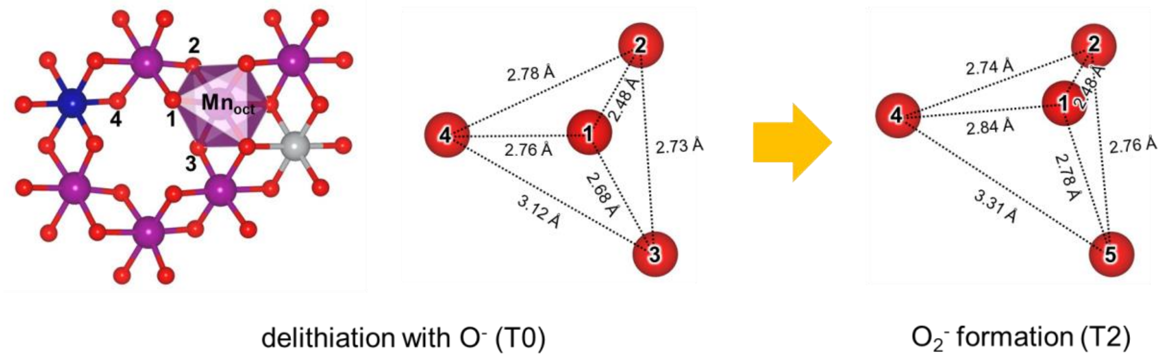

Supplementary Figure 9. The size of the threshold tetrahedral site between two octahedral sites for Mn in-plane migration (at x = 1.21). The O-O distances composing tetrahedral lines are compared before and after the superoxide formation.

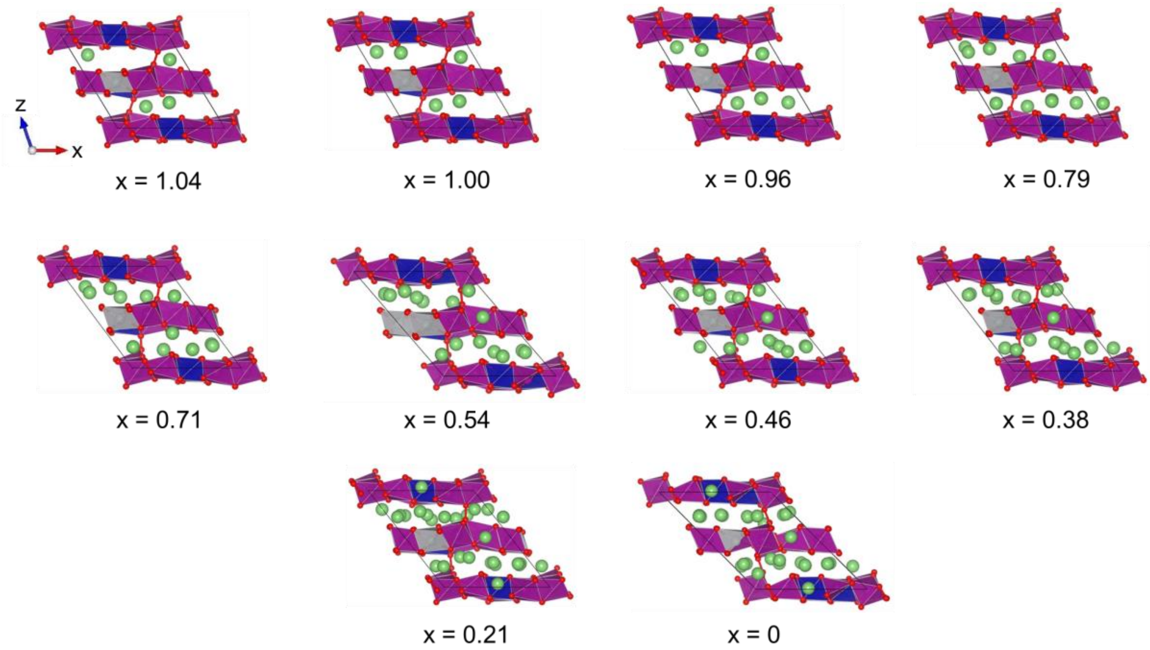

Supplementary Figure 10. Discharged structures at the charge state x = 1.04.

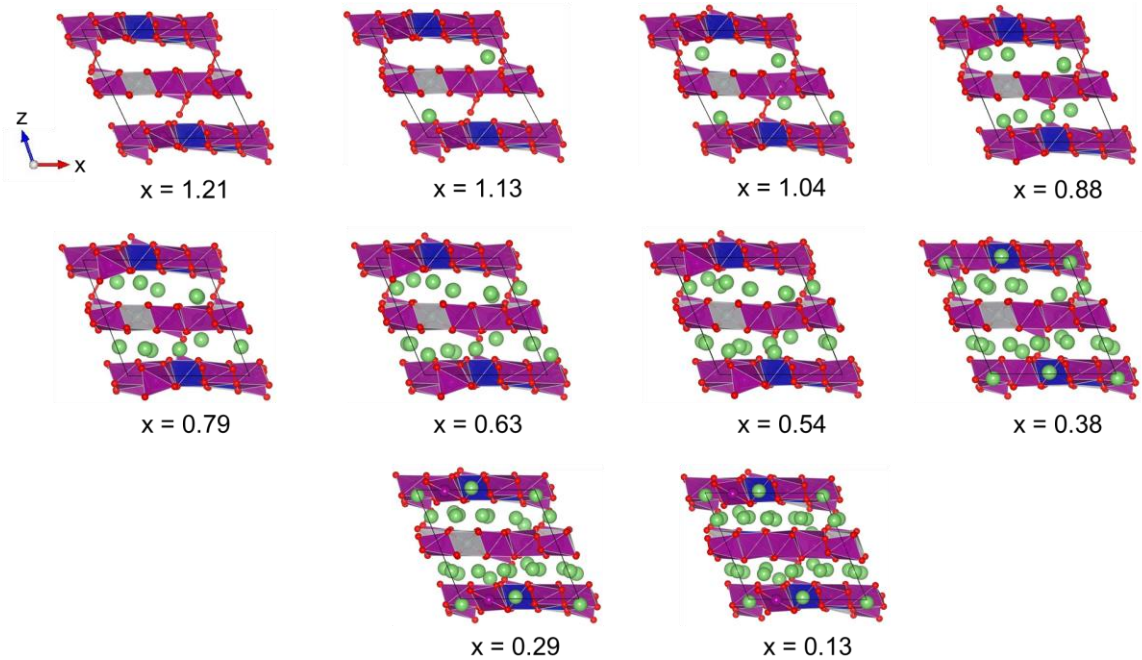

Supplementary Figure 11. Discharged structures at the charge state x = 1.21.

Supplementary Table 1. Magnetic moments, bond lengths and electronic configurations of different O-O dimer forms.

	$2O^{2-}$	$2O^{-}$	O_2^{2-}	O_2^{-}	O_2^{0}
Magnetic moment (μ_B)	0	1	0	1	2
$d_{O\text{-}O}$ (Å)	> 1.60	> 1.60	1.36 ~ 1.60	1.25 ~ 1.36	1.20 ~ 1.25
Electronic configuration